J. Microbiol. Biotechnol. (2010), **20**(7), 1061–1068
doi: 10.4014/jmb.1001.01018
First published online 18 May 2010

JOURNAL OF MICROBIOLOGY AND BIOTECHNOLOGY

Synthesis of Biosurfactant-Based Silver Nanoparticles with Purified Rhamnolipids Isolated from *Pseudomonas aeruginosa* BS-161R

Kumar, C. Ganesh[1]*, Suman Kumar Mamidyala[1], Biswanath Das[2], B. Sridhar[3], G. Sarala Devi[3], and Mallampalli SriLakshmi Karuna[4]

[1]Chemical Biology Laboratory, [2]Organic Chemistry Division, [3]Inorganic and Physical Chemistry Division, and [4]Lipid Science and Technology Division, Indian Institute of Chemical Technology, Uppal Road, Hyderabad 500 607, Andhra Pradesh, India

Received: January 18, 2010 / Revised: April 25, 2010 / Accepted: April 29, 2010

The biological synthesis of nanoparticles has gained considerable attention in view of their excellent biocompatibility and low toxicity. We isolated and purified rhamnolipids from *Pseudomonas aeruginosa* strain BS-161R, and these purified rhamnolipids were used to synthesize silver nanoparticles. The purified rhamnolipids were further characterized and the structure was elucidated based on one- and two-dimensional ^{1}H and ^{13}C NMR, FT–IR, and HR–MS spectral data. Purified rhamnolipids in a pseudoternary system of *n*-heptane and water system along with *n*-butanol as a cosurfactant were added to the aqueous solutions of silver nitrate and sodium borohydride to form reverse micelles. When these micelles were mixed, they resulted in the rapid formation of silver nanoparticles. The synthesized nanoparticles were characterized by UV–Visible spectroscopy, transmission electron microscopy, and energy dispersive X-ray spectroscopy (EDS). The nanoparticles formed had a sharp adsorption peak at 410 nm, which is characteristic of surface plasmon resonance of the silver nanoparticles. The nanoparticles were monodispersed, with an average particle size of 15.1 nm (σ=±5.82 nm), and spherical in shape. The EDS analysis revealed the presence of elemental silver signal in the synthesized nanoparticles. The formed silver nanoparticles exhibited good antibiotic activity against both Gram-positive and Gram-negative pathogens and *Candida albicans*, suggesting their broad-spectrum antimicrobial activity.

Keywords: *Pseudomonas*, rhamnolipid, biosurfactant, silver nanoparticles, antimicrobial

The intrinsic properties of noble metals such as silver, gold, and platinum have been considered advantageous in the synthesis of nanoparticles, which have become the center of attraction in the area of biotechnology. The growing environmental concerns and the strict environmental regulations in various countries and demand for developing clean, non-toxic, and eco-friendly synthetic approaches (green chemistry) in the synthesis of these nanoparticles has led to the fabrication of bio-based advanced materials. Biomineralization leading to the production of magnetite nanoparticles by magnetotactic bacteria [31], synthesis of silica nanospheres by diatoms [25], and bacterial cell surface layers (S-layers) found in a wide range of bacteria and archaea that synthesize gypsum and $CaCO_3$ layers [49] are good examples in this direction. Many microorganisms including bacteria, actinomycetes, and fungi have been explored for the synthesis of nanoparticles [34, 44]. The stabilization of the nanoparticles has been reported to be due to the proteins, reducing agents such as nitrate reductase [13], naphthoquinones [32], and anthraquinones [4] secreted by these organisms.

Much of the earlier work on the fabrication of nanoparticles is based primarily on physicochemical methods. Synthetic surfactants such as amine and carboxylate surfactants [28], cationic cetylpyridinium, or anionic sodium dodecyl sulfate, or nonionic Brij 56 [54] have also been used for nanoparticle synthesis. These surfactants are tensioactive molecules, amphipathic in nature with both hydrophilic and hydrophobic moieties, and exhibit surface-active properties. Many microorganisms like bacteria, fungi, yeasts, and algae are good sources of biosurfactants and have several advantages over their chemical counterparts; they are less toxic and biodegradable [37]. Low toxicity, better environmental compatibility, high foaming property, and high selectivity and specific activity at extreme conditions like pH, temperature and salinity make these biosurfactants as potential candidates, for a wide range of applications including microbial enhanced oil recovery (MEOR), bioremediation, medicine, pharmaceuticals, gene delivery system, cosmetics, food, and beverages [12, 42]. The use of surfactin, a lipopeptide-type

*Corresponding author
Phone: +91-40-27193105; Fax: +91-40-27193189;
E-mail: cgkumar@iict.res.in, cgkumar1@rediffmail.com

biosurfactant, has been recently reported in the preparation of polycaprolactone/montmorillonite nanocomposites [26]. In the present study, we used purified rhamnolipids produced by a newly isolated *Pseudomonas aeruginosa* strain BS-161R for the synthesis of biosurfactant-based monodispersed silver nanoparticles.

Materials and Methods

Isolation and Identification of the Bacterial Strain

Petroleum-contaminated sludge samples were collected from the Petroleum Refinery Unit, Essar Oil Limited, Vadinar, Jamnagar, Gujarat, India. These samples were transported to the laboratory in sterile sample bottles and stored at 4°C until further use. The samples were enriched in mineral salts medium [8] supplemented with *N*-hexadecane [1% (v/v)] for 3 weeks, and the bacterial strain was isolated using the methylene blue–CTAB method [47] and deposited in the in-house culture collection as BS-161R. The strain, which was found to be a good biosurfactant producer, was maintained on nutrient agar slants at 4°C and was also preserved as glycerol stocks in 25% glycerol stored at −70°C.

The isolate BS-161R was identified based on morphological, physiological, and biochemical characteristics following the methods described in *Bergey's Manual of Systematic Bacteriology* [24], and 16S rDNA gene sequencing was performed with universal bacterial primers such as the forward primer 27f (5'-AGA GTT TGA TCM TGG CTC AG-3') and the reverse primer 1525r (5'-AAG GAG GTG WTC CAR CC-3'). The amplified 1.5 kb PCR product was eluted from the agarose gel using the QIA quick gel extraction kit and gene sequencing was performed commercially (Vimta Labs Limited, Genome Valley, Shameerpet, Hyderabad, India). The 16S rDNA sequence of strain BS-161R were sequenced and deposited in the NCBI database under the Genbank accession number FJ940905.

Media and Fermentation Conditions

The isolate BS-161R was precultured aerobically to prepare a seed culture for mass production at 35°C in a 1,000-ml Erlenmeyer flask containing 250 ml of Bushnell–Hass mineral salts medium and agitated at 150 rpm for 24 h in an Ecotron shaker (Infors AG, Switzerland). A 3% (v/v) seed culture (optical density of about 2) was inoculated into 5 l of glycerol polypeptone broth (production medium) containing (in g/l) glycerol (30), polypeptone (5), meat extract (5), and NaCl (5), pH 7.5. Fermentation was carried out at 35°C for 72 h in a 7-l BIOFLO 410 bioreactor (New Brunswick Scientific, Edison, NJ, U.S.A.) with working volume of 5 l with agitation at 150 rpm and aeration of 0.5 vvm. The fermented medium was later subjected to centrifugation (SORVALL RC 5C Plus; Kendro Lab Products, Ashville, NC, U.S.A.) at 8,000 rpm to obtain a cell-free supernatant.

Surface-Active Properties

The surface tension of the culture supernatant was measured by the Wilhelmy plate method with a Du–Nouy tensiometer (K100MK2 Processor Tensiometer; Krüss, Hamburg, Germany). The concentration series was generated automatically with a computer-controlled Dosimat (Metrohm AG, Switzerland). The corresponding measurements and their evaluation were performed with the LabDesk software interfaced with the tensiometer. The critical micelle concentration (CMC) was measured by plotting the concentration of the surfactant as a function of surface tension, and the CMC was taken as the point where the slope of the curve abruptly changed [46]. The CMC was computed using the CMC add-in feature of LabDesk software of the tensiometer.

The emulsification index (EI_{24}) was determined by adding 4 ml of the culture supernatant to 6 ml of different compounds, such as *N*-hexadecane, toluene, xylene, mineral oil, and olive oil, individually, and the mixtures were vortexed at high speed for 2 min and then allowed to settle for 24 h before the emulsion stability was measured [11]. The EI_{24} was estimated after 24 h as the height of the emulsified layer expressed as a percentage of the total height of the liquid column.

Extraction, Purification, and Quantification of Rhamnolipids

The cell-free supernatant was acidified with 2 N HCl to pH 2 and extracted with ethyl acetate (1:1 ratio, 3 times). The extracted fractions were combined and evaporated to dryness under reduced pressure in a rotary vacuum evaporator (Rotavapor R-205; Büchi, Bern, Switzerland). Rhamnolipids (RL) from the extract were purified on a silica gel (100–200 mesh, 30×2 cm) column washed with chloroform and then eluted with 1–3% methanol in chloroform to remove traces of contaminants. The rhamnolipids as RL-1 and RL-2 were eluted with 4% and 7% methanol in chloroform, respectively. The active fractions were analyzed by thin-layer chromatography (TLC) on silica gel 60 plates (F_{254}; Merck, Darmstadt, Germany) in a mobile phase consisting of 20% methanol in chloroform. The plates were developed by spraying with phosphomolybdic acid reagent followed by heating at 100°C for 5 min. The pure rhamnolipids were obtained after vacuum evaporation of the solvents and lyophilized. The quantification of rhamnolipids in the supernatant was estimated with the orcinol method [9] and absorbance was measured at 420 nm using rhamnose as the standard.

Structural Characterization of Rhamnolipids

Nuclear magnetic resonance (NMR) spectra were recorded on a Bruker Avance 300 MHz NMR spectrometer (Bruker, Switzerland). The one-dimensional ^{1}H and ^{13}C NMR spectra and the two-dimensional NMR spectroscopy based on HMBC, HSQC, COSY, TOCSY, and ROESY were determined in deuterated chloroform at room temperature, and chemical shifts were represented in δ values expressed in ppm with tetramethylsilane (TMS) as an internal standard. The Fourier transform infrared spectrum (FT–IR) was performed using the Thermo-Nicolet Nexus 670 FT–IR spectrophotometer (Thermo Fisher Scientific Inc., Madison, WI, U.S.A.) using KBr pellets and spectra were collected at a resolution of 4 cm^{-1} in the wave number region of 400–4,000 cm^{-1}. The high resolution mass spectra (HR–MS) were recorded on a QSTAR XL Hybrid ESI-Q TOF mass spectrometer (Applied Biosystems Inc., Fosters City, CA, U.S.A.).

Rhamnolipid-Based Synthesis of Silver Nanoparticles

The silver nanoparticle synthesis was achieved with a purified rhamnolipid mixture used separately to form reverse micelles with 0.01 M aqueous silver nitrate or 0.1 M aqueous sodium borohydride ($NaBH_4$) solutions. The reaction was carried out by mixing 0.5 ml of 0.01 M aqueous silver nitrate, 3.0 g of purified rhamnolipids, 1.5 g of *n*-butanol, and 0.5 g of *n*-heptane together and stirring vigorously at room temperature until homogeneous reverse micelles were formed.

A second reaction mixture consisted of the similar quantities of solvents, rhamnolipids, and 0.1 M of aqueous $NaBH_4$ instead of aqueous $AgNO_3$. The two samples of reverse micelles were mixed and stirred on a magnetic stirrer for 1 h. During the process, the color of the colloidal mixture changed from colorless to brown. The silver nanoparticles were extracted from the reverse micelles by the addition of ethanol (0.5 ml of ethanol for 1 ml of reverse micelles) and the precipitated silver nanoparticles were separated from the solution by centrifugation at 10,000 rpm for 10 min. The nanoparticles were redispersed in water and then characterized.

Characterization of Silver Nanoparticles

The UV–Visible spectrum of the silver nanoparticles was recorded from 300 to 800 nm on a UV–Visible double-beam spectrophotometer (Lambda 25; Perkin-Elmer, Shelton, CT, U.S.A.). The morphological analysis of the silver nanoparticles was done by using transmission electron microscopy (TEM). A drop of the reaction mixture was placed over carbon-coated copper grids and the solvent was allowed to dry. Images were acquired on a Philips Technai-FE 12 TEM (120 KV). The energy dispersive X-ray spectroscopy (EDS) analysis was performed by scanning electron microscopy (SEM) with a Model S-520 (Hitachi, Japan) equipped with an EDS detector (Model: Oxford LINK-ISIS 300). The microanalyzer has qualitative, quantitative, imaging, and element mapping capabilities. The EDS spectrum was measured at 10 kV accelerating voltage.

Antimicrobial Susceptibility Testing of Silver Nanoparticles

Antimicrobial activity of the silver nanoparticles was determined by using the microtiter broth dilution method [3]. Different indicator strains employed were *Escherichia coli, Bacillus subtilis, Klebsiella planticola, Pseudomonas aeruginosa, Staphylococcus aureus,* and *Candida albicans*. Müller–Hinton broth was used as the diluent for bacterial strains, and potato dextrose broth for *Candida albicans*. Approximately 10^7 CFU/ml cells was inoculated and the final volume in each microtiter plate well was 0.1 ml. After incubation for 24 h at 35°C, the microtiter plates were read at 450 nm using the TRIAD multimode reader (Dynex Technologies, Inc., Chantilly, VA, U.S.A.) prior to and after incubation to determine the minimum inhibitory concentration (MIC) values. The MIC is defined as the lowest concentration of the compound that inhibited 90% of the growth when compared with that of the control growth.

RESULTS AND DISCUSSION

Identification of the Rhamnolipid Producing Strain

The isolated strain BS-161R formed smooth, circular colonies and produced a diffusible, fluorescent light-greenish pigment on pyocyanin agar plates. The growing cells were Gram-negative, strictly aerobic, asporogeneous, motile with one flagellum, and rod-shaped, having the size of 0.3–0.5×0.6–1.7 μm. Strain BS-161R grew well at pH 5–12 with an optimum at pH 7.5, but was inhibited at pH <5.0. Growth was observed between 10 and 41°C with an optimum at 35°C±2°C, but not above 45°C. It could tolerate up to 70 g/l NaCl in basal medium. The analysis of the 16S rDNA sequence of strain BS-161R was carried out using the BLASTN program, and the comparison of BLAST hits of 16s rDNA sequences exhibiting significant alignment is shown in the Supplementary data (Table ST1). Based on the 16S rDNA sequencing and the phenotypic properties, strain BS-161R was identified as *Pseudomonas aeruginosa*.

Crude Rhamnolipid Production and Characterization

When the isolate *Pseudomonas aeruginosa* BS-161R was cultivated under submerged conditions at 35°C in glycerol–polypeptone medium with 3% (w/v) glycerol, 1.5 g/l of the biosurfactant was produced after 96 h of incubation. The surface tension of the culture medium decreased to a maximum extent of 26.5 mN/m after 72 h of incubation. Furthermore, the CMC of the crude biosurfactant produced by the strain BS-161R was estimated as 66.884 mg/l, when the surface tension was 26.7 mN/m and revealed excellent surface active properties, which is in agreement with the published literature on biosurfactants that are reported to exhibit a wide range of CMC values ranging between 50 and 230 mg/l [1, 30]. It was observed that the crude biosurfactant showed good emulsification activity (EI_{24} value) ranging between 60% and 70% with all hydrocarbons studied (data not shown). The biosurfactant in the culture supernatant was also able to form stable emulsions.

Purification of the Rhamnolipids

Aqueous media using solvent systems that include ethyl acetate [51], $CHCl_3$–MeOH [2:1 (v/v)] [39], and Et_2O [20] have previously been reported for the isolation of rhamnolipids. After preliminary tests, ethyl acetate was used as an extraction solvent for the present study. In order to improve the extraction yield of rhamnolipids, the culture supernatant was initially acidified to pH 2 prior to extraction. This converts the rhamnolipids to a protonated form, makes them less soluble in water, and enables easy recovery of rhamnolipids with a subsequent ethyl acetate extraction step. The extracted rhamnolipids were purified using silica gel column chromatography. Thin-layer chromatography (TLC) (Supplementary data; Fig. S1) of the fractions after treatment with phosphomolybdic acid reagent revealed the presence of three major spots; the spot A was identified as a pigment, phenazine-1-carboxylic acid (PCA), with R_f value of 0.63, and spots B and C were rhamnolipids with R_f values of 0.4 and 0.24, respectively. The purified rhamnolipids were light yellow viscous liquids with solubility in most of the organic solvents but sparingly soluble in water.

Structural Characterization of the Purified Biosurfactants

The chemical structure of the purified biosurfactants was elucidated based on the NMR, FT–IR, and mass spectral data analyses. The one-dimensional ^1H NMR and ^{13}C NMR spectroscopies and FT–IR analysis revealed that both the compounds were glycolipids. The ^1H and ^{13}C chemical

Table 1. ^{1}H and ^{13}C NMR spectral data of the purified rhamnolipids in $CDCl_3$.

Carbon number	Rhamnolipid 1 (RL-1)		Rhamnolipid 2 (RL-2)	
	$\delta^{1}H^{a}$	$\delta^{13}C^{a}$	$\delta^{1}H^{a}$	$\delta^{13}C^{a}$
C-1'	4.79	95.1	4.81	94.5
C-2'	3.74	71.2	3.68	79.7
C-3'	3.57	67.7	3.44	68.8
C-4'	3.33	73.5	3.34	72.5
C-5'	3.66	70.4	3.60	70.6
C-6'	1.19	17.2	1.14	17.4
C-1"	-	-	4.80	102.4
C-2"	-	-	3.77	70.6
C-3"	-	-	3.48	67.9
C-4"	-	-	3.29	73.4
C-5"	-	-	3.64	71.3
C-6"	-	-	1.12	17.4
C-1	4.20	71.6	4.08	72.4
C-2	2.34	39.5	2.28	39.5
C-3	-	171.4	-	171.4
COOH	-	174.1	-	173.8
CH_3	0.86	13.9	0.85	14.0
C-4	5.36	71.0	5.33	71.3
C-5	2.47	39.5	2.47	39.3
CH_2	1.20–1.35	22.5–34.5	1.19–1.73	22.6–34.5

[a]300 MHz, chemical shift in ppm.

shifts are shown in Table 1. Additionally, two-dimensional NMR spectroscopies based on HMBC, HSQC, COSY, TOCSY, and ROESY were employed for complete assignments of the glycolipid signals (data not shown). In the ^{13}C NMR spectrum, spot B fractions showed lipid signals of CH_2 from δ 22.5–34.5 and CH_3 at δ 13.9 and ester and carboxylic signals at δ 171.4 and δ 174.1. Similarly, spot C fractions showed lipid signals in the ^{13}C NMR spectrum at δ 14.0 (CH_3) and resonance at δ 22.6–34.5 corresponds to CH_2, and ester and carboxylic signals at δ 171.4 and δ 173.8 (Supplementary data; Fig. S2–S5). The 1D and 2D ^{1}H COSY spectra revealed the presence of characteristic spin systems corresponding to the two α-rhamnose and two β-hydroxy fatty acid moieties. The interconnections and sequence were established from the cross-peaks within the 2D multiple-bond ^{13}C–^{1}H correlation (HMBC) spectrum, which corresponded to the interactions through three bonds *via* the bridging oxygen atoms. The HMBC spectrum also enabled the unambiguous assignment of the ^{13}C signals and a clear distinction between the two carbonyl carbons. The 2D COSY spectrum revealed the presence of only one rhamnose moiety in the case of monorhamnolipid, and the characteristic signal of H-2 of the dirhamnolipid at 4.02 ppm was absent, whereas the characteristic signals of both fatty acid moieties were present. In both monorhamnolipid and dirhamnolipid, it is assumed that all sugar moieties have the normal absolute

Table 2. Some characteristic absorption peaks of functional groups in purified rhamnolipids.

Functional groups	Spot 1 (wave number, cm^{-1})	Spot 2 (wave number, cm^{-1})
-C=O	1,739	1,737
-O–H	3,391	3,388
-C–O (primary)	1,045	1,056
-C–O (secondary)	1,125	1,128
-C–H stretching	2,925	2,927
-C–H stretching in methyl and methylene groups	2,854	2,857
-C–H bending	1,460 & 1,382	1,457 & 1,385

L-configuration, based on the integration of the 1D spectra provided and the information on the length of the fatty acid chains in both types of molecules. The ROESY analysis showed important signals: the space connection was obtained by the ROESY cross-peak at δ 4.683/4.074, which confirms the L-rhamnosyl(1'↔1)-hydroxyfatty acid linkage.

Based on the infrared spectra, some of the characteristic absorption peaks corresponding to the specific functional groups in the purified biosurfactant spots B and C are shown in Table 2 (Supplementary data; Fig. S6 and S7). The high resolution mass spectrometry (HR–MS) analysis under positive mode showed major molecular ion signals at *m/z* 527.3100 [$M+Na^+$] and 673.3790 [$M+Na^+$], corresponding to the sodium adduct of spots B and C, respectively (Supplementary data; Fig. S8 and S9). These ion signals were consistent with the structures expected for 2-*O*-α-L-rhamnopyranosyl-β-hydroxydecanoyl-β-hydroxydecanoic acid (Rha-C_{10}-C_{10}, a monorhamnolipid) and 2-*O*-α-L-rhamnopyranosyl-α-rhamnopyranosyl-β-hydroxydecanoyl-β-hydroxydecanoic acid (Rha-Rha-C_{10}-C_{10}, a dirhamnolipid), respectively, where Rha indicates a rhamnose moiety. All these results corroborate with the observations established for another biosurfactant produced by *Pseudomonas aeruginosa* DAUPE 614 [35]. In general, most *Pseudomonas* strains, when cultured on liquid medium containing glycerol or *n*-alkanes as carbon source, produced only two forms of rhamnolipids; namely, monorhamnolipid and dirhamnolipid [17, 18]. Syldatk *et al.* [51, 52] detected two more rhamnolipids that contained only one β-hydroxydecanoic acid unit, Rha-C_{10} and Rha-Rha-C_{10}, when resting cells of *Pseudomonas* sp. DSM 2874 were cultured on *n*-alkanes or glycerol. The mono- and dirhamnolipids, however, predominately represent 90% of all rhamnolipids produced by most *Pseudomonas* strains, and the present *Pseudomonas aeruginosa* BS-161R strain under study also produced only these two rhamnolipids.

Synthesis and Characterization of the Silver Nanoparticles

Rhamnolipids have a hydrophilic–lipophilic balance (HLB) value of 22–24, which means that they have a great

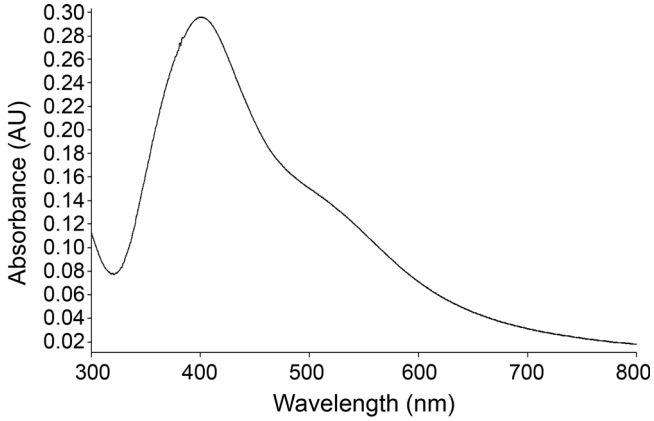

Fig. 1. UV–Visible absorbance spectrum of silver nanoparticles synthesized using a purified rhamnolipid mixture.

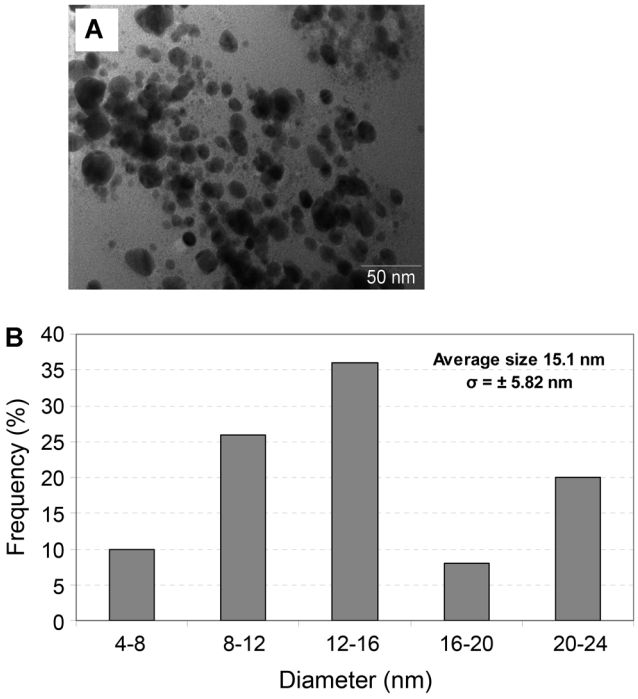

Fig. 2. TEM micrograph of silver nanoparticles using purified rhamnolipid mixture (**A**), and particle size distribution histogram of the silver nanoparticles measured from the TEM micrograph (**B**).

solubilization effect, but difficulty to form water-in-oil microemulsions (or reverse micelles) in an *n*-heptane and water system. Linear alcohols with different chain lengths can form two distinct polar and nonpolar parts and confer the amphiphilic character to the molecule, which acts as a cosurfactant. The effect of different chain-length alcohols on the phase behavior of microemulsions formed by a rhamnolipid was earlier demonstrated [53]. The mixing of rhamnolipids/*n*-heptane/water system with a linear alcohol such as *n*-butanol as a cosurfactant produced a pseudoternary system that greatly enhanced the formation of a single-phase microemulsion. The optimum HLB of this pseudoternary system ranged between 12.0 and 12.7 [6]. Thus, rhamnolipids can form reverse micelles similar to or even better than other surfactants [16, 43]. This concept of reverse micelle formation using rhamnolipids was explored for the synthesis of silver nanoparticles. The UV–Visible absorbance spectrum (Fig. 1) of silver nanoparticles after synthesis in reverse micelles and extraction by the addition of ethanol exhibited a sharp absorption peak at 410 nm, which corresponds to the resonance of the silver nanoparticles and might arise as a result of the surface plasmon vibration in the silver nanoparticles. The particle aggregation trend occurring because of extraction yields a variation of the width and the red-shift of the maximum in the absorption spectrum [40]. The rhamnolipids in the reaction milieu act as capping agents and stabilize the silver nanoparticles by forming a steric hindrance around the particles, and the aggregation of the nanoparticles is prevented mostly by electrostatic interactions. It is well established that surface plasmon resonances (SPR) dominate the optical absorption spectra of metal nanoparticles, which shift to longer wavelengths with increase in particle size [7], and the absorbance of silver nanoparticles depends on size and shape [21, 50]. In general, the number of SPR peaks decrease as the symmetry of the nanoparticle increases [50]. Mock *et al*. [33] correlated the absorption spectra of individual silver nanoparticles with their size (40–120 nm) and shape (spheres, decahedrons, triangular truncated pyramids and platelets) determined by TEM. They found that spherical and roughly spherical nanoparticles, decahedral or pentagonal nanoparticles, and triangular truncated pyramids and platelets absorb in the blue, green, and red parts of the spectrum, respectively. In all these cases, the SPR peak wavelength increased with size, as expected. In the present study, the TEM micrograph revealed that the silver nanoparticles are monodispersed and spherical in shape (Fig. 2A). Based on the particle size distribution histogram (Fig. 2B) evaluated from the corresponding TEM micrograph, the average size of nanoparticles was computed as 15.1 nm (σ=±5.82 nm) with a narrow size distribution. The energy dispersive X-ray spectroscopy analysis (Fig. 3) revealed the elemental composition profile of the synthesized nanoparticles, which indicated the presence of elemental silver signal.

Antimicrobial Susceptibility Testing

The antimicrobial activity of silver nanoparticles (Table 3) was evaluated against various pathogenic reference strains including Gram-positive and Gram-negative bacteria and *Candida albicans*. The 15-nm-sized silver nanoparticles, synthesized using a purified rhamnolipid mixture exhibited a lowest minimum inhibitory concentration of 7.81 μg/ml against both Gram-negative and Gram-positive bacteria like

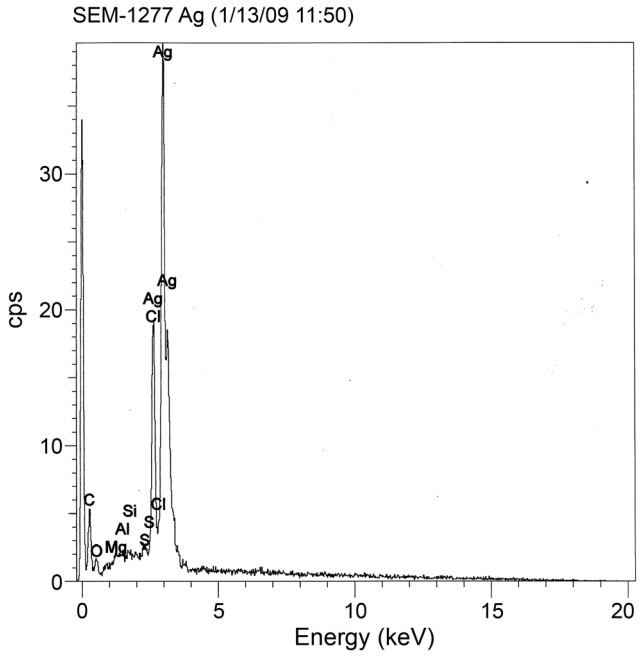

Fig. 3. Energy dispersive X-ray (EDS) spectrum of the silver nanoparticles.

Escherichia coli, *Klebsiella planticola*, and *Staphylococcus aureus*, and also against *Candida albicans*, suggesting the broad-spectrum nature of their antimicrobial activity. Reports suggest that the antimicrobial activity of silver nanoparticles may be due to the attachment to the cell membrane, penetration into the bacteria, and damage of the cell membrane with release of cell contents [38]. Another possibility would be the release of silver ions from the nanoparticles, which may contribute to the bactericidal properties of silver nanoparticles. In contrast to the bactericidal effects of silver, the antimicrobial activity of silver nanoparticles was also influenced by the dimensions of the particles; the smaller the particle size, the greater the antimicrobial effect [5, 36]. It is known that silver and its compounds exhibited strong inhibitory and bactericidal properties against a wide spectrum of bacteria and fungi [10, 27, 48].

Table 3. Antimicrobial activity of the silver nanoparticles synthesized using a purified rhamnolipid mixture.

S. No.	Indicator strain(s)	MIC[a] (μg/ml)
1	*Escherichia coli* MTCC 739	7.81
2	*Klebsiella planticola* MTCC 530	7.81
3	*Bacillus subtilis* MTCC 121	15.62
4	*Staphylococcus aureus* MTCC 2940	7.81
5	*Pseudomonas aeruginosa* MTCC 2453	15.62
6	*Candida albicans* MTCC 3017	7.81

[a]MIC, Minimum inhibitory concentration.
Tests were repeated three times and average values are shown.

Silver nanoparticles, apart from gaining special attention as new-generation antimicrobial agents [23, 41], have been used lately in a wide range of healthcare products, such as burn dressings, scaffolds, vascular grafts, human skin and medical devices [15, 22, 29], bone cement [2], biolabeling [45], removal of microorganisms on textile fabrics [14], and in water purification systems [19]. In view of the growing importance of silver nanoparticles in various biomedical and biotechnological applications, we have developed a method to synthesize nanoparticles using biosurfactant-based silver nanoparticles by using purified rhamnolipids isolated from the culture filtrates of *Pseudomonas aeruginosa* BS-161R.

Acknowledgments

The authors thank the Director, IICT and Dr. Ahmed Kamal, Division of Organic Chemistry for extending the facilities to carry out this research work. The authors acknowledge the financial assistance provided in the form of a Senior Research Fellowship by the Council of Scientific and Industrial Research (CSIR), New Delhi to Mr. S. K. Mamidyala. The authors wish to thank Prof. V. Lakshmipati for his kind help in editing, and valuable comments during the preparation of the manuscript. The authors also thank Mr. N. Kishtam Raju and Maji Shyama, Petroleum Refinery Unit, Essar Oil Limited, Vadinar, Jamnagar, Gujarat, India for extending their help in collection of the sludge samples from the refinery.

References

1. Abalos, A., A. Pinazo, M. R. Infante, M. Casals, F. Garcia, and A. Manresa. 2001. Physicochemical and antimicrobial properties of new rhamnolipids by *Pseudomonas aeruginosa* AT10 from soybean oil refinery wastes. *Langmuir* **17:** 1367–1371.
2. Alt, V., T. Bechert, P. Steinrücker, M. Wagener, P. Seidel, E. Dingeldein, E. Domann, and R. Schnettler. 2004. An *in vitro* assessment of the antibacterial properties and cytotoxicity of nanoparticulate silver bone cement. *Biomaterials* **25:** 4383–4391.
3. Amsterdam, D. 1996. Susceptibility testing of antimicrobials in liquid media, pp. 52–111. *In* Loman, V. (ed.). *Antibiotics in Laboratory Medicine*, Fourth Edition. Williams and Wilkins, Baltimore, MD.
4. Baker, R. A. and J. H. Tatum. 1998. Novel anthraquinones from stationary cultures of *Fusarium oxysporum. J. Ferment. Bioeng.* **85:** 359–361.
5. Baker, C., A. Pradhan, L. Pakstis, J. D. Pochan, and S. I. Shah. 2005. Synthesis and antibacterial properties of silver nanoparticles. *J. Nanosci. Nanotechnol*. **5:** 244–249.
6. Bourrel, M. and R. S. Schechter. 1988. *Microemulsions and Related Systems: Formulation, Solvency and Physical Properties*. Marcel Dekker, New York.

7. Brause, R., H. Moeltgen, and K. Kleinermanns. 2002. Characterization of laser ablated and chemically reduced silver colloids in aqueous solution by UV/VIS spectroscopy and STEM/SEM microscopy. *Appl. Phys. B Lasers Optics* **75:** 711–716.
8. Bushnell, L. D. and H. F. Hass. 1941. The utilization of certain hydrocarbons by microorganisms. *J. Bacteriol.* **41:** 653–673.
9. Chandrasekaran, E. V. and J. N. Bemiller. 1980. Constituent analyses of glycosamino-glycans, pp. 89–96. *In* R. L. Whistler (ed.). *Methods in Carbohydrate Chemistry*. Academic Press Inc., New York.
10. Cho, K. H., J. E. Park, T. Osaka, and S. G. Park. 2005. The study of antimicrobial activity and preservative effects of nanosilver ingredient. *Electrochim. Acta* **51:** 956–960.
11. Cooper, D. G. and B. G. Goldenberg. 1987. Surface-active agents from two *Bacillus* species. *Appl. Environ. Microbiol*. **53:** 224–229.
12. Desai, J. D. and I. M. Banat. 1997. Microbial production of surfactants and their commercial potential. *Microbiol. Mol. Biol. Rev.* **61:** 47–64.
13. Duran, N., P. D. Marcato, O. L. Alves, G. I. de Souza, and E. Esposito. 2005. Mechanistic aspects of biosynthesis of silver nanoparticles by several *Fusarium oxysporum* strains. *J. Nanobiotechnol*. **3:** 8.
14. Falletta, E., M. Bonini, E. Fratini, A. Lo Nostro, G. Pesavento, A. Becheri, P. Lo Nostro, P. Canton, and P. Baglioni. 2008. Clusters of poly(acrylates) and silver nanoparticles: Structure and applications for antimicrobial fabrics. *J. Phys. Chem. C* **112:** 11758–11766.
15. Furno, F., K. S. Morley, B. Wong, B. L. Sharp, P. L. Arnold, S. M. Howdle, *et al*. 2004. Silver nanoparticles and polymeric medical devices: A new approach to prevention of infection? *J. Antimicrob. Chemother*. **54:** 1019–1024.
16. Garti, N., A. Aserin, and M. Fanun. 2000. Non-ionic sucrose esters microemulsions for food applications. Part 1: Water solubilization. *Colloids Surf. A* **164:** 27–38.
17. Hisatsuka, K., T. Nakahara, N. Sano, and K. Yamada. 1971. Formation of rhamnolipid by *Pseudomonas aeruginosa* and its function in hydrocarbon fermentation. *Agric. Biol. Chem*. **35:** 686–692.
18. Itoh, S., H. Honda, F. Tomita, and T. Suzuki. 1971. Rhamnolipids produced by *Pseudomonas aeruginosa* grown on *n*-paraffin (mixture of C_{12}, C_{13}, and C_{14} fractions). *J. Antibiot*. **24:** 855–859.
19. Jain, P. and T. Pradeep. 2005. Potential of silver nanoparticle-coated polyurethane foam as an antibacterial water filter. *Biotechnol. Bioeng*. **90:** 59–63.
20. Jain, D. K., H. Lee, and J. T. Trevors. 1992. Effect of addition of *Pseudomonas aeruginosa* UG2 inocula or biosurfactants on biodegradation of selected hydrocarbons in soil. *J. Ind. Microbiol*. **10:** 87–93.
21. Kerker, M. 1985. The optics of colloidal silver: Something old and something new. *J. Colloid Interface Sci*. **105:** 297–314.
22. Kim, S. and H. J. Kim. 2006. Anti-bacterial performance of colloidal silver treated laminate wood flooring. *Int. Biodeterior. Biodegradation* **57:** 155–162.
23. Kim, K.-J., W. S. Sung, B. K. Suh, S.-K. Moon, J.-S. Choi, J. G. Kim, and D. G. Lee. 2009. Antifungal activity and mode of action of silver nano-particles on *Candida albicans. Biometals* **22:** 235–242.
24. Krieg, N. R. and J. G. Holt. 1989. Gram-negative rods and cocci, pp. 140–219. *In* J. G. Holt (ed.). *Bergey's Manual of Systematic Bacteriology*. Williams and Wilkins, Baltimore, MD.
25. Kröger, N., R. Deutzmann, and M. Sumper. 1999. Polycationic peptides from diatom biosilica that direct silica nanosphere formation. *Science* **286(5442):** 1129–1132.
26. Liao, H.-T. 2008. A new application of biosurfactant for the preparation of polycaprolactone/layered silicate nanocomposites. *Polym. Eng. Sci.* **48:** 1524–1531.
27. Lok, C. N., C. M. Ho, R. Chen, Q. Y. He, W. Y. Yu, H. Sun, P. K. Tam, J. F. Chiu, and C. M. Chen. 2006. Proteomic analysis of the mode of antibacterial action of silver nanoparticles. *J. Proteome Res*. **5:** 916–924.
28. Malik, A. S., M. J. Duncan, and P. G. Bruce. 2003. Mesostructured iron and manganese oxides. *J. Mater. Chem.* **13:** 2123–2126.
29. Maneerung, T., S. Tokura, and R. Rujiravanit. 2008. Impregnation of silver nanoparticles into bacterial cellulose for antimicrobial wound dressing. *Carbohydr. Polym*. **72:** 43–51.
30. Mata-Sandoval, J., J. Karns, and A. Torrents. 1999. High-performance liquid chromatography method for the characterization of rhamnolipids mixture produced by *Pseudomonas aeruginosa* UG2 on corn oil. *J. Chromatogr*. **864:** 211–220.
31. Matsunaga, T., T. Suzuki, M. Tanaka, and A. Arakaki. 2007. Molecular analysis of magnetotactic bacteria and development of functional bacterial magnetic particles for nano-biotechnology. *Trends Biotechnol*. **25:** 182–188.
32. Medentsev, A. G. and V. K. Alimenko. 1998. Naphthoquinone metabolites of the fungi. *Phytochemistry* **47:** 935–959.
33. Mock, J. J., M. Barbic, D. R. Smith, D. A. Schultz, and S. Schultz. 2002. Shape effects in plasmon resonance of individual colloidal silver nanoparticles. *J. Chem. Phys.* **116:** 6755–6759.
34. Mohanpuria, P., N. K. Rama, and S. K. Yadav. 2008. Biosynthesis of nanoparticles: Technological concepts and future applications. *J. Nanopart. Res.* **10:** 507–517.
35. Monteiro, S. A., G. L. Sassaki, L. M. de Souza, J. A. Meira, J. M. de Araujo, D. A. Mitchell, L. P. Ramos, and N. Krieger. 2007. Molecular and structural characterization of the biosurfactant produced by *Pseudomonas aeruginosa* DAUPE 614. *Chem. Phys. Lipids* **147:** 1–13.
36. Morones, J. R., J. L. Elechiguerra, A. Camacho, K. Holt, J. B. Kouri, J. T. Ramírez, and M. J. Yacaman. 2005. The bactericidal effect of silver nanoparticles. *Nanotechnology* **16:** 2346–2353.
37. Nitschke, M., S. G. V. A. O. Costa, and J. Contiero. 2005. Rhamnolipid surfactants: An update on the general aspects of these remarkable biomolecules. *Biotechnol. Prog.* **21:** 1593–1600.
38. Panacek, A., L. Kvitek, R. Prucek, M. Kolar, R. Vecerova, N. Pizurova, V. K. Sharma, T. Nevecna, and R. Zboril. 2006. Silver colloid nanoparticles: Synthesis, characterization, and their antibacterial activity. *J. Phys. Chem. B* **110:** 16248–16253.
39. Parra, J. L., J. Pastor, F. Comelles, M. A. Manresa, and M. P. Bosch. 1990. Studies of biosurfactants obtained from olive oil. *Tenside Surf. Det*. **27:** 302–306.
40. Qi, L., Y. Gao, and J. Ma. 1999. Synthesis of ribbons of silver nanoparticles in lamellar liquid crystals. *Colloids Surf. A* **157:** 285–294.
41. Rai, M., A. Yadav, and A. Gade. 2009. Silver nanoparticles as a new generation of antimicrobials. *Biotechnol. Adv.* **27:** 76–83.

42. Rodrigues, L., I. M. Banat, J. Teixeira, and R. Oliveira. 2006. Biosurfactants: Potential applications in medicine. *J. Antimicrob. Chemother.* **57:** 609–618.
43. Rodriguez, C. and D. P. Acharya. 2003. Effect of ionic surfactants on the phase behavior and structure of sucrose ester/water/oil systems. *J. Colloid Interface Sci.* **262:** 500–505.
44. Sastry, M., A. Ahmad, M. I. Khan, and R. Kumar. 2004. Microbial nanoparticle production, pp. 126–135. *In* C. M. Niemeyer and C. A. Mirkin (eds.). *Nanobiotechnology.* Wiley-VCH, Weinheim, Germany.
45. Schrand, A. M., L. K. Braydich-Stolle, J. J. Schlager, L. Dai, and S. M. Hussain. 2008. Can silver nanoparticles be useful as potential biological labels? *Nanotechnology* **19**: 235104.
46. Sheppard, J. D. and C. N. Mulligan, 1987. The production of surfactin by *Bacillus subtilis* grown on peat hydrolysate. *Appl. Microbiol. Biotechnol*. **27:** 110–116.
47. Siegmund, I. and F. Wagner. 1991. New method for detecting rhamnolipids excreted by *Pseudomonas* species during growth on mineral agar. *Biotechnol. Tech.* **5:** 265–268.
48. Silver, S. 2003. Bacterial silver resistance: Molecular biology and uses and misuses of silver compounds. *FEMS Microbiol. Rev.* **27:** 341–353.
49. Sleytr, U. B., C. Huber, N. Ilk, D. Pum, B. Schuster, and E. M. Egelseer. 2007. S-Layers as a tool kit for nanobiotechnological applications. *FEMS Microbiol. Lett*. **267:** 131–144.
50. Sosa, I. O., C. Noguez, and R. G. Barrera. 2003. Optical properties of metal nanoparticles with arbitrary shapes. *J. Phys. Chem. B* **107:** 6269–6275.
51. Syldatk, C., S. Lang, and F. Wagner. 1985. Chemical and physical characterization of four interfacial-active rhamnolipids from *Pseudomonas* sp. DSM 2874 grown on alkanes. *Z. Naturforsch.* **40c:** 51–60.
52. Syldatk, C., S. Lang, U. Matulovic, and F. Wagner. 1985. Production of four interfacial active rhamnolipids from *n*-alkanes or glycerol by resting cells of *Pseudomonas* species DSM 2874. *Z. Naturforsch.* **40c:** 61–67.
53. Xie, Y., Y. Li, and R. Ye. 2005. Effect of alcohols on the phase behaviour of microemulsions formed by a biosurfactant – rhamnolipid. *J. Dispersion Sci. Technol.* **26:** 455–461.
54. Yuan, Z.-Y., T.-Z. Ren, and B.-L. Su. 2004. Surfactant-mediated nanoparticle assembly of catalytic mesoporous crystalline iron oxide materials. *Catal. Today* **93–95:** 743–750.